Original Article *Journal of Sustainability and Environmental Management (JOSEM), Vol. 3, No. 3 (2024), 129 – 137*
p-ISSN 2822-1729, e-ISSN 2822-1737 Available online at https://www.nepjol.info/index.php/josem

Enhancing Severe Weather Prediction Over Myanmar Using INSAT-3D Sounder and Hyperspectral Satellite Observations

Thet Mar Soe[1,3], Fangmin Zhang[1*], Pradeep Thapliyal[2], Kyaw Lwin Oo[3], Tin Mar Htay[3]

[1]Collaborative Innovation Center on Forecast and Evaluation of Meteorological Disasters, Nanjing University of Information Science and Technology, Nanjing, China
[2]Centre for Space Science and Technology Education in Asia and the Pacific (CSSTEAP), India
[3]Department of Meteorology and Hydrology, Myanmar

*Corresponding author: fmin.zhang@nuist.edu.cn

Abstract: This study investigates the application of INSAT-3D Sounder and hyperspectral sounders from polar-orbiting satellites (AIRS, IASI, and CrIS) in predicting severe weather over Myanmar, with a focus on two severe weather case studies from Rakhine State. Data on the stability index (Lifted Index, LI) and Total Precipitable Water (TPW) from INSAT-3D and hyperspectral sounders were analyzed following the methodology of Schmit et al. (2009). The workflow involved downloading data from various sources (MOSDAC, NCDC, Mirador) and generating LI and TPW images. Numerical values for specific stations were extracted, followed by time series analysis. Results demonstrated that increasing LI values, indicating atmospheric instability, and TPW values exceeding 50 mm were critical predictors of severe weather with a lead time of 3–4 hours. These findings suggest that LI and TPW are valuable indicators for nowcasting severe weather. However, the study also highlighted limitations in temporal resolution due to the observation gaps from polar-orbiting sounders. Future research aims to integrate Himawari-8/9 AHI data with hyperspectral sounder observations to improve nowcasting accuracy and the development of a robust tool for severe weather and thunderstorms in Myanmar.

Keywords: *INSAT-3D, Myanmar, TPW, Weather*

Conflicts of interest: None
Supporting agencies: None

Received 11.04.2024; Revised 04.11.2024; Accepted 26.11.2024

Cite This Article: Soe, T.M., Fangmin, Z., Thapliyal, P., Oo, K.L., & Htay, T.M. (2024). Enhancing Severe Weather Prediction Over Myanmar Using INSAT-3D Sounder and Hyperspectral Satellite Observations. *Journal of Sustainability and Environmental Management*, 3(3), 129-137.

1. Introduction

The Earth's climate is complex, with components and feedback processes operating on different time scales. The atmosphere controls many feedback processes, including radiation with clouds, water vapor, precipitation, and temperature. Understanding the properties of the atmosphere is crucial for understanding processes within the atmosphere and feedback mechanisms among the entire climate system. Atmospheric sounding provides high spatial and temporal resolution of temperature and moisture parameters, which are required for nowcasting, short-range weather forecasting, and input for NWP models. Satellites like Atmospheric Infrared Sounder (AIRS), Microwave Limb Sounder (MLS), and GPS Radio Occultation provide these parameters with reasonable accuracy. The Indian National Satellite System (INSAT-3D) and INSAT-3DR have gained significance due to their geostationary orbit, providing high temporal resolution profiles of temperature and water vapour. These data are expected to play an important role in the prediction of numerical weather over India and its surroundings.

1.1. Myanmar and its climate

The Republic of Myanmar is situated in the Western portion of mainland Southeast Asia, between the latitudes 9° 32'N to 28° 31' N and longitudes 92° 10' to 101° 11' E. The area of Myanmar's territory is 676,575 km², stretching 930 km from west to east and 2050 km from north to south. Myanmar borders India to the Northwest, Bangladesh to the west Laos to the East, China to the North-Northeast, Thailand to the Southeast, the Andaman Sea, and the Bay of Bengal to the South. The majority of people in Myanmar are living in rural areas. Myanmar is a mountainous country. Myanmar slopes from north to south, from an elevation of 19,296 feet (5,881 metres) at Mount Hkakabo (the country's highest peak) in the extreme north to sea level at the Irrawaddy (Ayeyarwady) and Sittaung (Sittoung) river deltas. The mountain ranges generally run from north to south. The country as a whole can be divided into five physiographic regions—the northern mountains, the western ranges, the eastern plateau, the central basin and lowlands, and the coastal plains.

The climate of Myanmar varies depending on location, elevation, and elevation in the highlands. The climate is tropical and has three seasons: a "cool winter from November to February, a hot summer season in March and April, and a rainy season from May to October, dominated by the southwest monsoon" (Lwin, 2002; Oo, 2023; Sein, Zhi, et al., 2021). A large portion of the country lies between the Tropic of Cancer and the Equator and the entirety of the country lies in the monsoon region of Asia, with its coastal regions receiving over 5,000 mm (196.9 in) of rain annually. Annual rainfall in the delta region is approximately 2,300 mm (94.82 in), while average annual rainfall in the Dry Zone in central Myanmar is less than 1,000 mm (39.4 in) (Aung et al., 2017). The higher elevations of the highlands are predisposed to heavy snowfall, especially in the North. The Northern regions of Myanmar are the coolest, with average temperatures of 21 °C. Coastal and delta regions have an average maximum temperature of 32 °C (Sein, Ullah, et al., 2021).

Figure 1: Republic of Myanmar

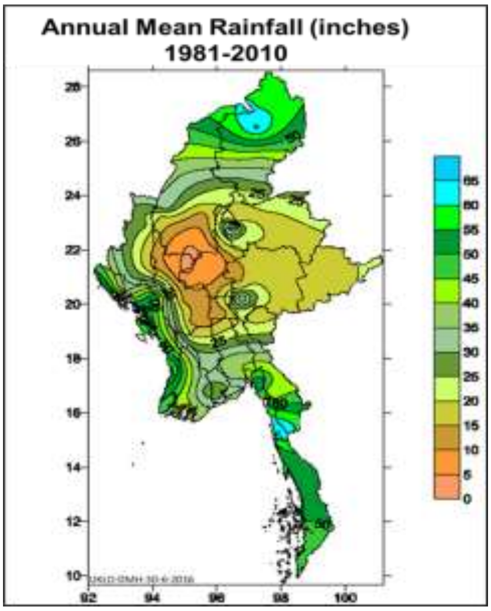

Figure 2: Rainfall Distribution over Myanmar

This study evaluates the effectiveness of the INSAT-3D Sounder and hyperspectral sounders from polar-orbiting satellites (AIRS, IASI, and CrIS) in predicting severe weather conditions over Myanmar. By analyzing stability indices such as the Lifted Index (LI) and Total Precipitable Water (TPW) in two case studies, the study aims to assess the complementary strengths of these sounders, explore their respective limitations, and propose improvements for nowcasting severe weather events, particularly in enhancing lead time and spatial coverage.

2. Data Used and Methodology

2.1. Data used

Satellite data corresponding to two case studies have been downloaded from various websites. The details of the data are provided in the table-10.

Table 1: Details of the data used

Sensor name / Data	*Source*	*Spatial Resolution*	*Temporal Resolution*	*format*
INSAT-3D Imager L1C Product	www.mosdac.gov.in	4 Km	Half-Hourly	HDF5
INSAT-3D Sounder L2B Products	www.mosdac.gov.in	10 Km	Hourly	HDF5
AIRS Sounder L2 Product	www.mirador.gsfc.nasa.gov	50 Km	0630-0830/ 1830-2030 UTC	HDF5

CrIS Sounder L2 Products	www.ncdc.noaa.gov	50 Km	0500-0700/ 1700-1900 UTC	NetCDF
IASI Sounder L2 Product	www.ncdc.noaa.gov	50 Km	0200-0400/ 1400-1600 UTC	NetCDF

2.2. Area of study

In this project we have selected area as shown in Figure 3 below. Four Met stations located in this area are selected for the study and same is shown in Table 2 below.

Figure 3: Area of study

Table 2: Rainfall (mm) over selected cases for the Study Area

Date/ Station	MAUNGDAW	KYAUKTAW	SITTWE	KYAUKPHYU
Case-1: 13 MAY 18	41	11	3	5
Case-2: 22 Apr 17	23	41	2	0

The INSAT-3D Imager data, which have a high spatial resolution of 4 km and a temporal resolution of 30 minutes, were used to study the evolution and approach of weather over the above-mentioned stations for selected cases. Thereafter, LI and TPW were studied to identify the changes in atmospheric thermodynamic structure that led to the development of severe weather over the area of study.

Case-1: In the first case, the severe weather conditions started at 0800 UTC on 13 May 2018, and the time of severe weather cessation was 1200 UTC on the same day. Large rain was observed over Maungdaw (41.0 mm) followed by Kyauktaw (11 mm).

Case-2: In the second case, the severe weather conditions started at 0800 UTC on 22 April 2017, and the time of severe weather cessation was 1700 UTC on the same day. Large rain was observed over Maungdaw (23 mm) and Kyauktaw (41 mm).

2.3. Atmospheric parameter used for study

Lifted Index: Galway (1956) developed the lifted index to predict instability. It is defined as the difference between the environmental temperature at 500mb and the temperature of the air parcel at 500mb when it is lifted at this level (500mb) pseudo-adiabatically (Schmit et al., 2002).

$$LI = (T500)_{environment} - (T500)_{parcel}$$

The range of values of LI for the chance of the development of the severe storms is given in the following table:

Table 7: Threshold values of LI

Lifted Index (LI) Range (°C)	Chance of Storm
> 2	No significant activity
-2 < LI < 2	Thunderstorm Possible
-4 < LI < -2	Thunderstorms more probable
LI > -4	Severe thunderstorms possible

Total Precipitable Water (TPW): TPW is computed from the retrieved atmospheric moisture profiles and represents the total integrated moisture in the atmospheric column from the surface to the top of the atmosphere. This parameter provides useful information to weather forecasters and hydrologists to improve their situational awareness for a number of situations that require forecasting of events, such as heavy rain, flash flooding. The TPW also serves to initialize the moisture field used in numerical weather prediction models (Lee et al., 2019; Parihar et al., 2018).

Total precipitable water may be computed using the formula

$$TPw = \int_{p_1}^{p2} \frac{q}{g}\,dp \ldots\ldots\ldots\text{Equation 1}$$

where p1 and p2 are bounding pressures of surface (~1000 hPa) and top of the atmosphere (i.e., about 100 hPa beyond which water vapor amount is assumed to be in negligible), q – specific humidity in Kg/Kg, and unit of total precipitable water is mm depth of equal amount of liquid water above a surface of one square meter (if pressure is in Pa and specific humidity is in Kg/Kg).

2.4. Method details

Various studies in the recent past have discussed the importance of multi- and hyperspectral infrared sounders for nowcasting applications, particularly for the high impact events such as severe storms and thunderstorms (Li et al., 2011; Li et al., 2012; Menzel et al.,2018; Schmit et al., 2009, Weisz et al., 2015). Schmit et al. (2009) discussed the importance of high spectral resolution observations for nowcasting applications and compared these with the existing multispectral GOES Sounder and proposed hyperspectral sounder (HES) onboard GOES-R satellite. However, the HES was dropped from GOES-R, and hyperspectral-sounding observations remain available only from polar-orbiting satellites, such as AIRS, IASI, and CrIS. There are only two sounding instruments in geostationary orbit for providing continuous hourly atmospheric profiles useful for nowcasting, GOES-12/13/14 Sounder over the continental US (Menzel and Purdom, 1994) and INSAT-3D/3DR Sounder over the Indian region. Both GOES and INSAT-3D/3DR Sounder are similar multispectral sounders having 18 IR channels with low spectral resolution (10-100 cm-1) to profile the atmospheric temperature and humidity.

The fine-spectral-resolution sounder is capable of providing much greater vertical resolution of temperature, humidity, and trace gases with a very high accuracy comparable to those from radiosonde (Smith, 2009; Menzel et al., 2018). Besides accurate atmospheric profiles, the high-spectral-resolution sounder will also provide continuous 3-D moisture and wind profiles, important parameters for forecasting at different timescales. This will improve the monitoring of the mesoscale environment for severe weather forecasting and other applications.

Operational use of current GOES (Menzel & Purdom, 1994) and INSAT-3D Sounder include the following:

- Clear-sky radiances,
- Profiles of temperature and moisture,
- Atmospheric stability indices,
- Layer and total precipitable water (TPW),
- Cloud top retrievals (Pressure/Temperature/ Cloud amount),
- Surface skin temperature,
- Water vapor atmospheric motion vectors

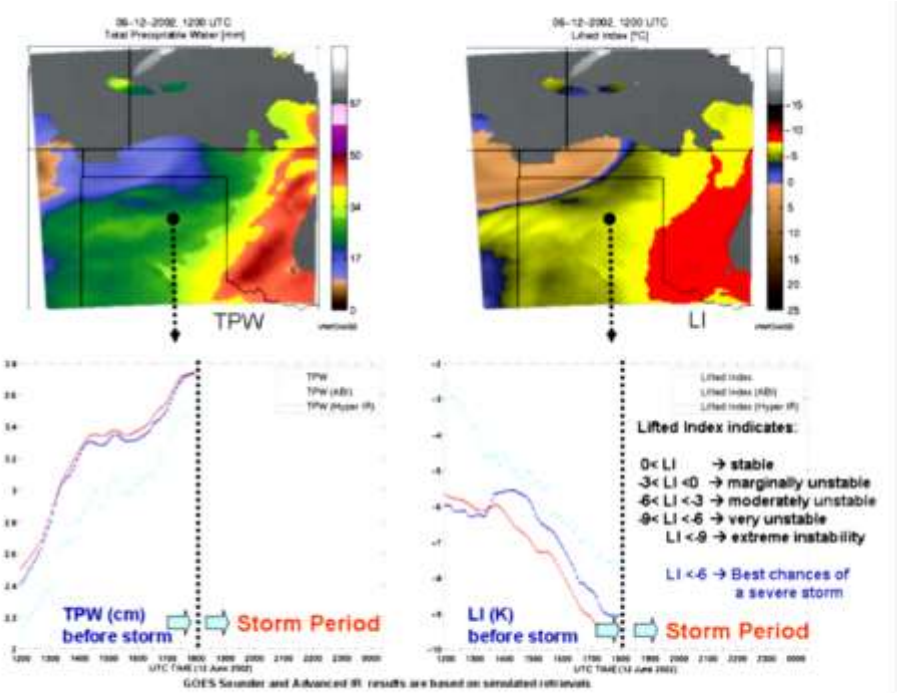

Figure 4 (a) top-left: truth-TPW (1200 UTC), (b) top-right: truth-LI (1200 UTC), (c) bottom-left: time evolution of TPW, and (d) bottom-right: time evolution of LI

Image analysis using high temporal resolution GEO sounder observations is important for Nowcasting (within 1-6 hr), especially forecasting severe thunderstorms by monitoring water vapor and atmospheric stability indices. Identifying regions of convective initiation has commercial benefits, especially in the aviation industry. More than half of the air traffic delays at U.S. airports are due to weather, and many of those delays are a response to convective weather. Better weather information would lead to a better flight planning process. Benefits are estimated to be larger than U.S. $25 million a year (as computed in 2002).

Schmit et al. (2009) used the output of the MM5 model to simulate HES (hyperspectral sounder) and ABI (pseudo multi-spectral sounder) radiances. The following geophysical products were retrieved and used for nowcasting:

- Lifted Index (LI)
- Total precipitable water (TPW)

Model fields were used as truth. Figure 1 shows a time sequence of LI and TPW from simulated ABI and HES data. The top-left panel shows Truth-TPW (1200 UTC), and the top right shows Truth-LI (1200 UTC). The bottom left panel shows the time evolution of TPW, and the bottom right panel shows the time evolution of LI. The HES observations show a close match with the Truth, whereas the ABI shows evolution properly but with small biases. This shows that by observing the temporal evolution of the TPW and LI, the initiation of thunderstorms can be predicted and monitored. In the absence of a GEO hyperspectral sounder, the multispectral GEO sounder can be used as the gradients of TPW and LI are large during the pre-storm period.

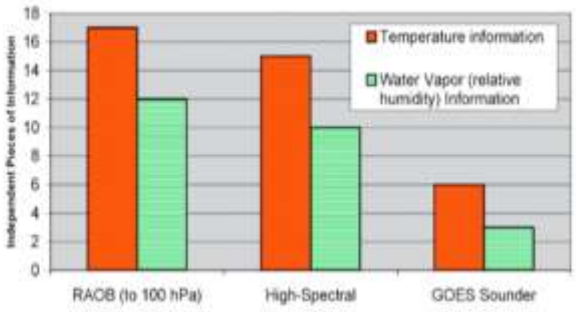

Figure 5: Information content analysis of the hyperspectral and multispectral sounders

Schmit et al. (2009) carried out a relative vertical information analysis (Fig.2) and demonstrated that a high-spectral resolution sounder (HES) has a much greater vertical resolving power of temperature and moisture than a low-spectral-resolution sensor (GOES Sounder). (Prunet et al., 1998) also carried out information content study of IASI and found that these radiance contain very high information contents comparable to the radiosonde. Although the in-situ nature of radiosondes enables their high vertical information content, these twice-a-day measurements, primarily over land, do not meet the temporal and spatial sampling requirements to monitor rapidly changing phenomena.

However, the increased number of hyperspectral sounders flown onboard polar orbiting satellites by various space agencies, e.g., AIRS, IASI-A/B, and CrIS, enable frequent observations over a particular location (Menzel et al., 2018). Keeping this in mind, the present work explores the use of simultaneous INSAT-3D/3DR sounder observations with available hyperspectral sounders for prediction of severe storms over Myanmar, which otherwise lacks ground-based radiosonde observations. Two case studies have been selected in the recent past, and satellite data from different instruments were acquired for these events. In the future, many space agencies plan to launch hyperspectral sounders onboard the GEO platform that will further improve nowcasting applications for severe weather conditions and thunderstorms (Schmetz et al., 2012; Schmit et al., 2009).

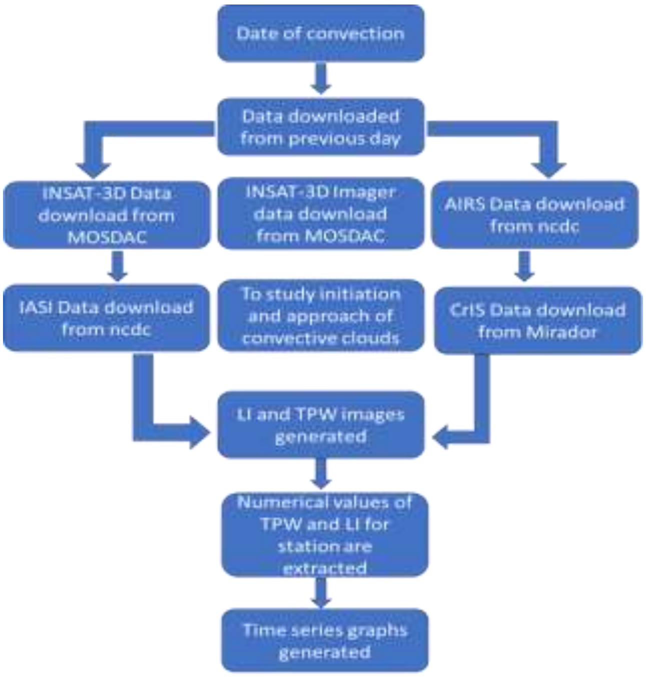

Figure 6: Flow chart of methodology

3. Results and discussion

The results and discussions are given in the form of case studies in the following subsections. Two cases have been selected based on data from meteorological stations. The details of the studied cases are as follows:

3.1. Case study

From the TIR1 images of the INSAT-3D Imager (Figure-15), it was clearly evident that cloudiness started developing at around 0200 UTC in the Bay of Bengal near the Rakhine coast. Another cloud mass approached from the NW, and finally, both these cells affected selected stations from around 0800 UTC till 1200 UTC. The amount of rainfall received by selected stations is shown in Table 9.

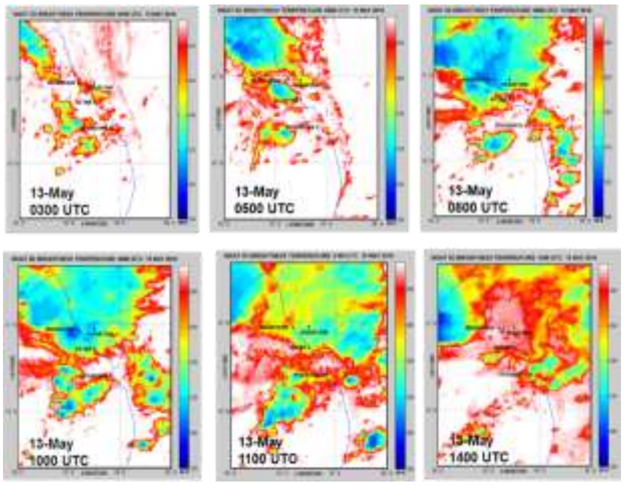

Figure 7: TIR1 Images from INSAT-3D Imager on 13 May 2018 depicting development of the severe storm

Thermodynamics of the System

Stability Indices are taken from INSAT-3D sounder-derived products, and computed from AIRS, IASI, and CrIS sounder profiles are plotted on a map (Figures 16 to 18) for the region of interest. The maps in Figure 16 show a comparison of LI from INSAT-3D during the pre-storm period with relatively clearer sky conditions with available hyperspectral sounder. Figure 17 shows the evolution of the lifted index before and after the storm period from available INSAT-3D sounder data. As the storm approaches the 4 stations, the cloudiness increases, and the lifted index products are not available in those cloudy sky regions. Contrary to this, the lifted index from hyperspectral sounder data is shown (figure 18) over the entire region of coverage due to a combination with microwave sounder data available from polar-orbiting satellites. These figures show that the values of the Lifted Index around the region of interest were -2 to -6 K on 12 May 2018 in INSAT-3D, whereas -6 to -8K by the hyperspectral sounder. However, on 13 May 2018, from 0200 UTC, the values became further negative around -8 to -10 in INSAT-3D as well as in hyperspectral sounders, which indicated an approach of severe weather. After 1400 UTC these values started increasing. INSAT-3D shows an increase of values in the range of 0 to -2.5 K. Similarly, other sounders also showed an increase of value in the range of 0 to -4. This increasing gradient is an indication of the weakening of storm weather conditions and subsequent improvement.

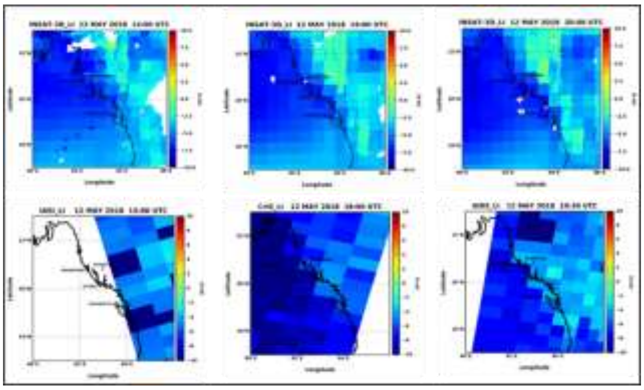

Figure 8: Combined INSAT-3D and Hyperspectral sounder plots for LI on 12 May 2018

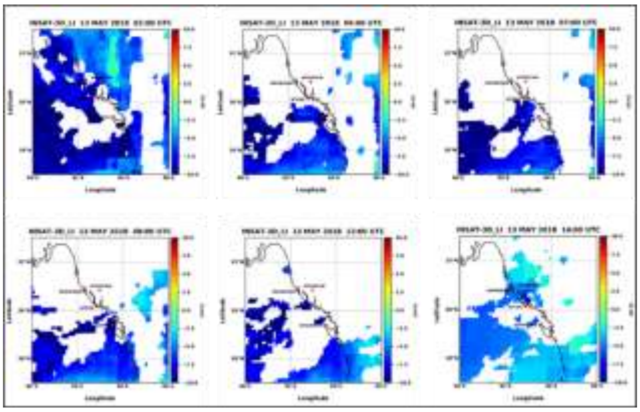

Figure 9: INSAT-3D sounder plots for LI on 13 May 2018

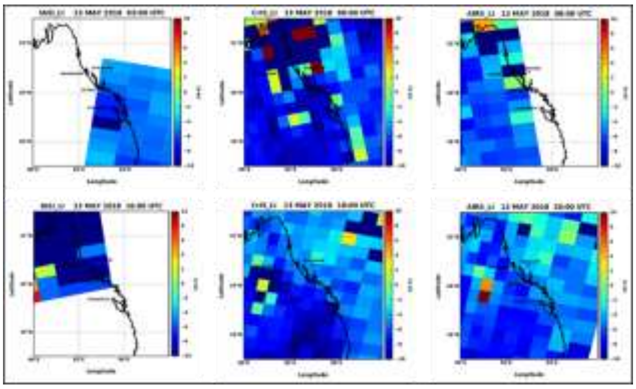

Figure 10: Hyperspectral sounder plots for LI on 13 May 2018

Time series of LI

LI values are extracted over four stations and then averaged out to calculate the LI over an area of interest. In this time series graph shown in figure-19, LI was plotted to see the changes that took place before the storm and after the storm. The graph indicates that LI continuously increased till the storm event and then subsequently decreased, which confirms the discussions with TIR1 images in the previous section. This figure clearly shows the importance of frequent observations from INSAT-3D

Sounder, with very few hyperspectral observations available even after combining AIRS, IASI, and CrIS data. There is also some mismatch between INSAT-3D Sounder and hyperspectral sounder observation, which may be due to the fact that spatial averaging in both sounding systems is kept separate due to the availability of respective observations. The software routine developed for the computation of the lifted index also needs to be validated and fine-tuned to provide accurate values.

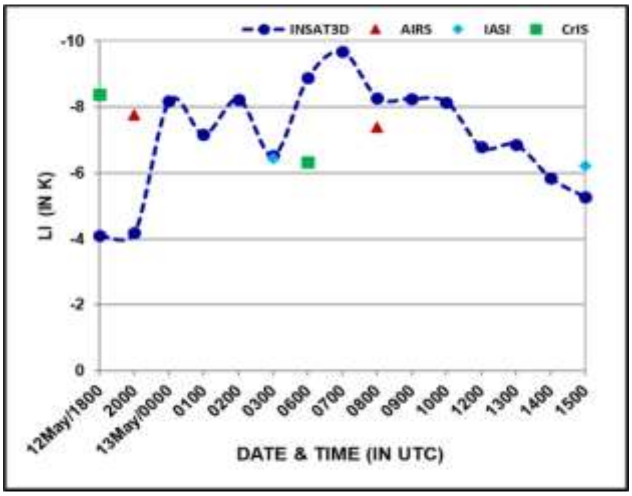

Figure 11: Time series of LI on 12 - 13 May 2018

Total precipitable water

The maps in Figure 20 show a comparison of TPW from INSAT-3D during the pre-storm period with relatively clearer sky conditions with available hyperspectral sounder. Figure 21 shows the evolution of TPW before and after the storm period from available INSAT-3D sounder data. As the storm approaches the 4 stations, the cloudiness increases, and the TPW products are not available in those cloudy sky regions. Contrary to this, the lifted index from hyperspectral sounder data is shown (figure 22) over the entire region of coverage due to a combination with microwave sounder data available from polar-orbiting satellites.

Figures 20 to 22 show that the values of TPW over the region of interest were 30 to 40 mm on 12 May 2018 in INSAT-3D, whereas 40 to 42 mm by hyperspectral sounder. However, on 13 May 2018, from 0200 UTC, the values became further higher, around 50 to 52 mm in INSAT-3D as well as in hyperspectral sounders, which was around 52 to 57 mm, which indicates approaching severe weather. After 1400 UTC these values started decreasing. INSAT-3D shows a decrease of values in the range of 38 to 40 mm. Similarly, hyperspectral sounders also showed a decrease in values in the range of 40 to 42. This decreasing gradient indicated the passing of severe weather conditions and subsequent improvement.

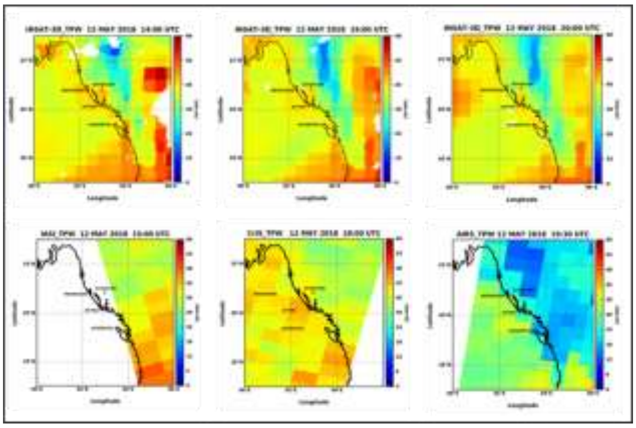

Figure 12: Combined INSAT-3D and Hyperspectral sounder plots for TPW on 12 May 2018

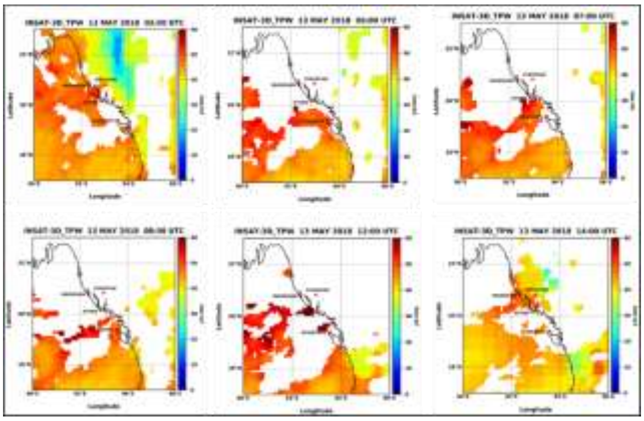

Figure 13: INSAT-3D sounder plots for TPW on 13 May 2018

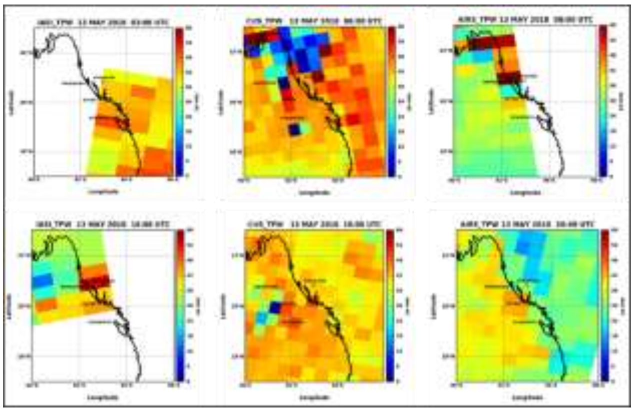

Figure 14: Hyperspectral sounder plots for TPW on 13 May 2018

Time series of TPW

TPW values are extracted over four stations and then averaged out to calculate the TPW values over an area of interest. In this time series graph shown in Figure 23, the TPW was plotted with time to see the changes that took place before the storm and after the storm. The graph indicated that TPW continuously increased till the storm event at 0800 UTC and then subsequently it decreased, which confirms the discussion with images in the previous section. This figure again clearly shows the importance of frequent observations from INSAT-3D Sounder, with very few hyperspectral observations available even after combining AIRS, IASI, and CrIS data. There is also some mismatch between INSAT-3D Sounder and hyperspectral sounder observation, which may be due to the fact that spatial averaging in both sounding systems is kept separate due to the availability of respective observations. However, one interesting fact emerges from this figure, and that is the contrast of TPW values, which coincidently pics up a high TPW value at ~0800 UTC very nicely. It is due to the fact that INSAT-3D Sounder employs a large area average to retain sufficient pixels for averaging as the TPW over cloudy pixels is not retrieved, whereas in hyperspectral sounder due to the use of combined microwave sounder, the TPW is retrieved over cloudy pixels as well, and therefore, the spatial averaging is done over smaller region around Met stations.

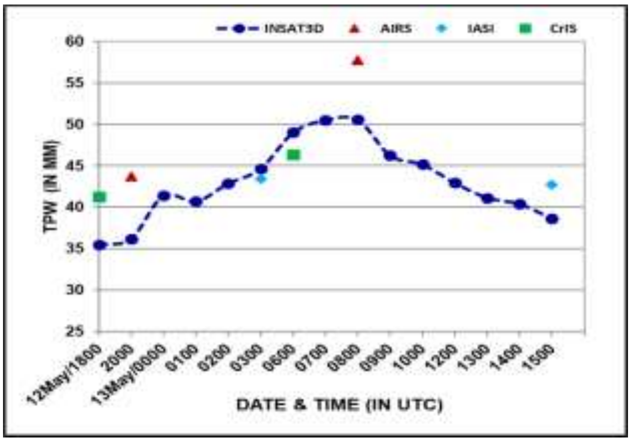

Figure 15: Time series of TPW on 12 and 13 May 2018

The comparison between INSAT-3D and hyperspectral sounders (AIRS, IASI, and CrIS) in forecasting severe weather over Myanmar shows complementary strengths (Gogoi et al., 2021). INSAT-3D provides high temporal resolution, capturing instability trends before storms but struggles with data retrieval in cloudy conditions. In contrast, hyperspectral sounders equipped with microwave sensors can consistently retrieve data even in cloudy regions, offering better spatial coverage during storm evolution (Rani & Prasad, n.d.). Both systems showed similar trends for Lifted Index (LI) and Total Precipitable Water (TPW), with more negative LI and increasing TPW leading up to storm events, followed by stabilization post-storm. Time series analysis highlighted these trends, with hyperspectral sounders providing more continuous data, while INSAT-3D offered frequent updates when clear sky conditions allowed (Parihar et al., 2018). The slight discrepancies between the two systems, particularly in pre-storm values, underscore the importance of integrating both for more accurate severe weather forecasting. Combining geostationary and polar-orbiting sounders enhances forecasting accuracy, making it a critical approach for effective nowcasting in regions like Myanmar (Satapathy & Jangid, 2018).

4. Conclusion

The study highlights the advantages of integrating data from INSAT-3D Sounder and hyperspectral sounders (AIRS, IASI, and CrIS) for improved severe weather forecasting over Myanmar. By analyzing thermodynamic stability indices such as the Lifted Index (LI) and Total Precipitable Water (TPW), the study demonstrates that combining geostationary and polar-orbiting observations enhances forecasting accuracy, particularly in pre-storm atmospheric assessments. The results confirm that LI and TPW serve as crucial indicators for convective storm prediction, with their time-series trends offering a lead time of 3–4 hours for severe weather warnings. Additionally, the ability of hyperspectral sounders to retrieve data over cloudy regions significantly improves observational coverage. While some discrepancies arise due to spatial averaging differences, the study emphasizes the potential of integrating multi-source satellite data for nowcasting applications. Future work should expand case studies and incorporate Himawari-8/9 AHI observations to develop a robust nowcasting tool for severe weather prediction in the region.

References

Aung, L. L., Zin, E. E., Theingi, P., Elvera, N., Aung, P. P., Han, T. T., Oo, Y., & Skaland, R. G. (2017). *Myanmar Climate Report*. Norwgian Meterological Institute, 9, 105.

Gogoi, R. B., Kundu, S. S., & Raju, P. L. N. (2021). Impact of INSAT-3D radiance data assimilation using WRF 3DVAR on simulation of Indian summer monsoon and high-resolution rainfall forecast over hilly terrain. *Natural Hazards*, *109(*1), 221–236. https://doi.org/10.1007/s11069-021-04833-3

Lee, Y., Han, D., Ahn, M. H., Im, J., & Lee, S. J. (2019). Retrieval of total precipitablewater from Himawari-8 AHI data: A comparison of random forest, extreme gradient boosting, and deep neural network. *Remote Sensing*, *11(*15), 1–18. https://doi.org/10.3390/rs11151741

Li, J., Li, J., Otkin, J., Schmit, T. J., & Liu, C. Y. (2011). Warning information in a preconvection environment from the geostationary advanced infrared sounding system-A simulation study using the IHOP case. *Journal of Applied Meteorology and Climatology*, *50(*3), 776–783. https://doi.org/10.1175/2010JAMC2441.1

Li, J., Liu, C. Y., Zhang, P., & Schmit, T. J. (2012). Applications of full spatial resolution space-based advanced infrared soundings in the preconvection environment. *Weather and Forecasting*, *27(*2), 515–524. https://doi.org/10.1175/WAF-D-10-05057.1

Lwin, T. (2002). The climate changes over Myanmar during the last decades. *Water Resources Journal*.

Menzel, W. P., & Purdom, J. F. W. (1994). Introducing GOES-I: the first of a new generation of geostationary operational environmental satellites. *Bulletin - American Meteorological Society, 75(*5), 757–781.

Oo, K. T. (2023). Climatology Definition of the Myanmar Southwest Monsoon (MSwM): Change Point Index (CPI). *Advances in Meteorology*, 2023, 2346975. https://doi.org/10.1155/2023/2346975

Parihar, S., Mitra, A. K., Mohapatra, M., & Bhatla, R. (2018). Potential of insat-3d sounder-derived total precipitable water product for weather forecast. Atmospheric *Measurement Techniques, 11(*11), 6003–6012. https://doi.org/10.5194/amt-11-6003-2018

Prunet, J.N. (1998). *The in- formation content of clear sky IASI radiances and their potential for numerical weather prediction*. https://doi.org/https://doi .org/10.1002/qj.49712454510.

Rani, S. I., & Prasad, V. S. (n.d.). *Simulation and Validation of INSAT-3D Sounder Radiance at NCMRWF.*

Satapathy, J., & Jangid, B. P. (2018). Monitoring a local extreme weather event with the scope of hyperspectral sounding. *Meteorology and Atmospheric Physics, 130(*3), 371–381. https://doi.org/10.1007/s00703-017-0523-z

Schmetz, J. ; Stuhlmann, R. ; Grandell, J. ; Tjemkes, S. ; Calbet X. ; Koenig, M. and, & Rota, S. (2012). *Meteosat Third Generation (MTG) development in the context of other future geostationary satellite observations*. Fall Meeting, San Francisco, CA, Amer. Geophys. Union.

Schmit, T. J., Feltz, W. F., Menzel, W. P., Jung, J., Noel, A. P., Heil, J. N., Nelson, J. P., & Wade, G. S. (2002). Validation and use of GOES sounder moisture information. *Weather and Forecasting, 17(*1), 139–154. https://doi.org/10.1175/1520-0434(2002)017<0139:VAUOGS>2.0.CO;2

Schmit, T. J., Li, J., Ackerman, S. A., & Gurka, J. J. (2009). High-spectral-and high-temporal-resolution infrared measurements from geostationary orbit. *Journal of Atmospheric and Oceanic Technology, 26(*11), 2273–2292. https://doi.org/10.1175/2009JTECHA1248.1

Sein, Z. M. M., Ullah, I., Syed, S., Zhi, X., Azam, K., & Rasool, G. (2021). Interannual variability of air temperature over myanmar: The influence of enso and iod. *Climate, 9(*2), 1–19. https://doi.org/10.3390/CLI9020035

Sein, Z. M. M., Zhi, X., Ullah, I., Azam, K., Ngoma, H., Saleem, F., Xing, Y., Iyakaremye, V., Syed, S., Hina, S., & Nkunzimana, A. (2021). Recent variability of subseasonal monsoon precipitation and its potential drivers in {Myanmar} using insitu observation during 1981--2020. *International Journal of Climatology, 42(*6), 3341–3359. https://doi.org/10.1002/joc.7419

Smith, W. (2009). Evolution, current capabilities, and advances in satellite ultra-spectral ir sounding. *AIP Conference Proceedings,* 1100(December 2008), 335–338. https://doi.org/10.1063/1.3116985.

© The Author(s) 2024. JOSEM is licensed under a Creative Commons Attribution-NonCommercial 4.0 International License.